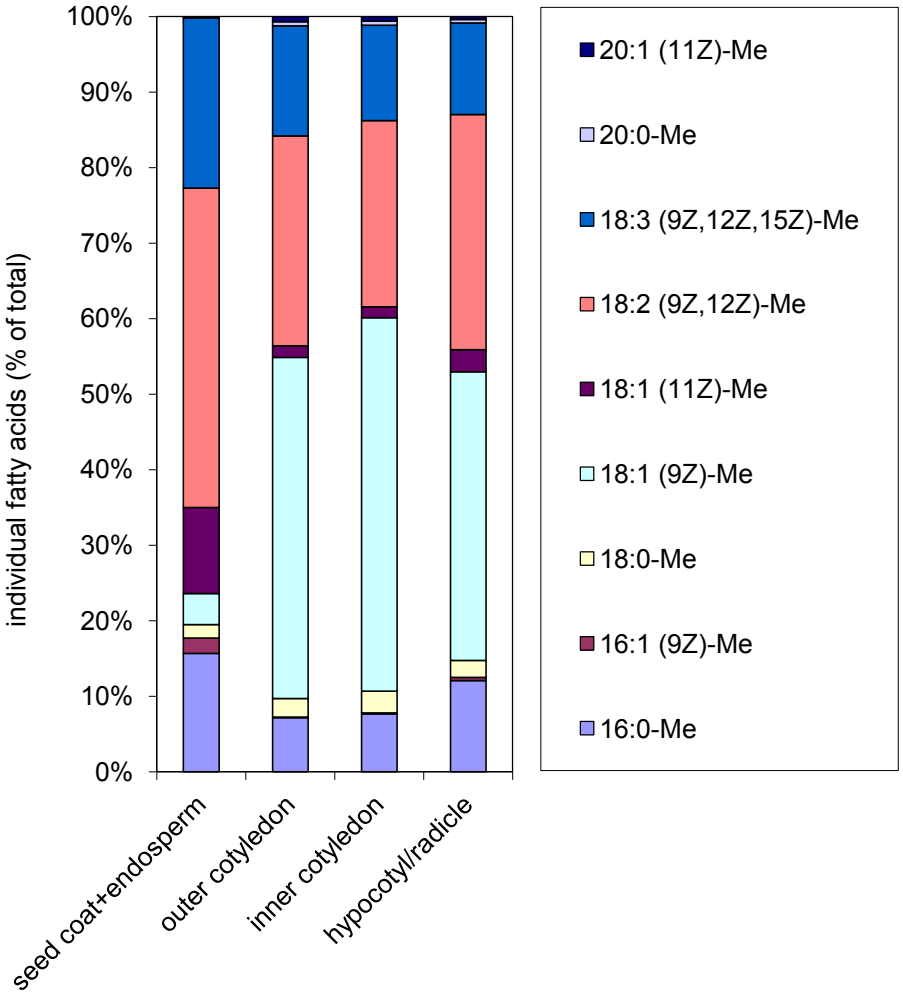

Supplemental Figure 1. Fatty acid profile of various seed organs in *B. napus* at mid storage stage; measured as fatty acid methyl esters using gas chromatography.

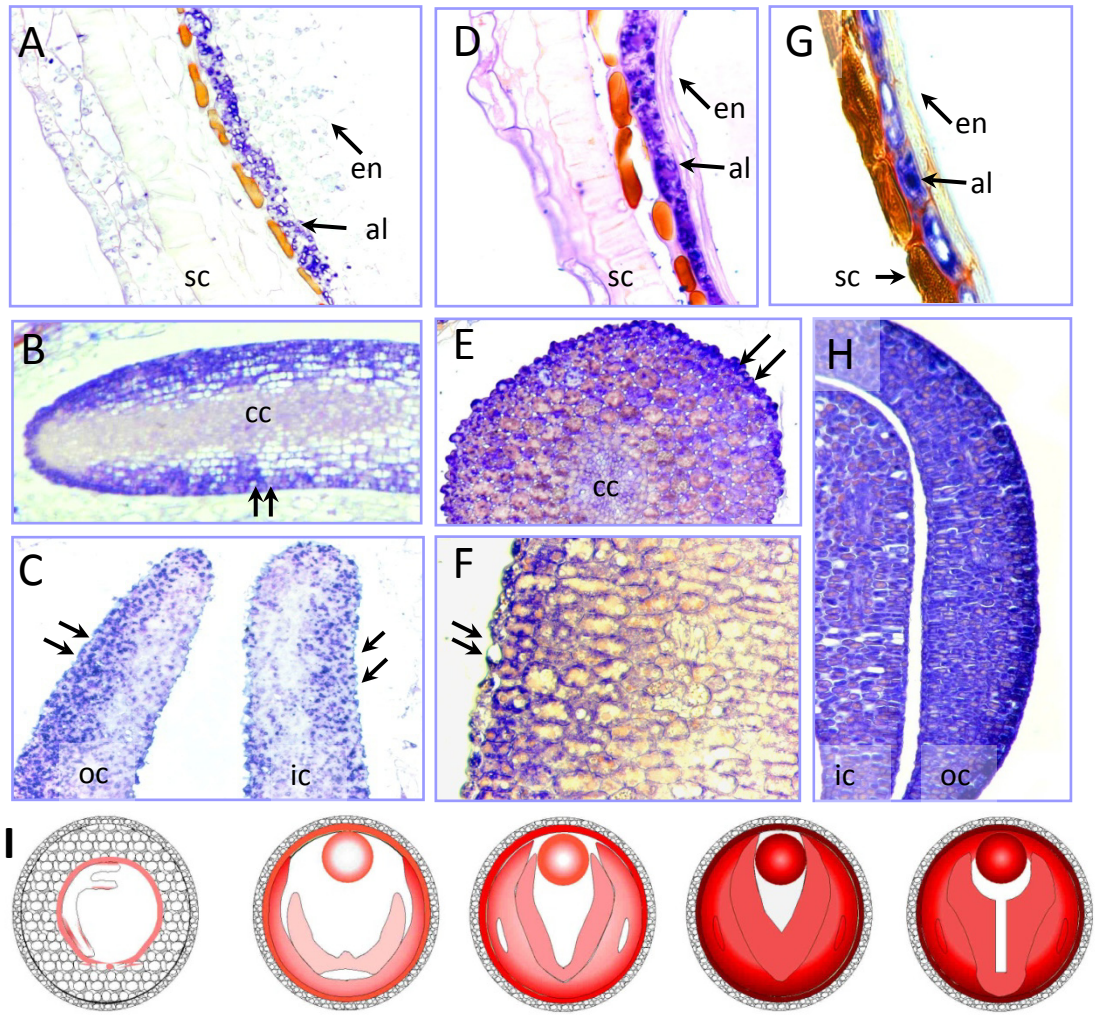

Supplemental Figure 2. Oleosin deposition in developing seeds of *B. napus*.

The same seeds analysed for their lipid distribution by MRI were also used to immunohistochemically locate the sites of oleosin deposition. Both the spatial and temporal distribution of the oil body protein oleosin overlapped that of the lipid.

(**A-C**) early stage: oleosin protein was detected in embryo and endosperm but not in seed coat. In endosperm, staining appeared strictly in peripheral (aleurone) cell layers (A). Accumulation of oleosin within the embryo started at the radicle (B), occupying parenchyma (cortex region, arrowed), and spread toward cotyledons. Cotyledons were stained starting from the base and mainly within abaxial region (arrowed in C).

(**D-F**) mid-stage: seed coat was not labelled, while aleurone of endosperm (D) and embryo were intensely stained. Labelling within the embryo was observed in radicle (arrowed in E). Both cotyledons were stained: outer cotyledon showed strong gradient with maximum within abaxial region (arrowed in F). Gradient within the inner cotyledon was less pronounced. Epidermis but not provascular tissues were labelled.

(**G-H**) late stage: labelling in aleurone layer of endosperm remained (G). In embryo, the intensity of labelling reached its maximum. Within outer cotyledon, a clear gradient in staining was observed with maximum in abaxial region (H). The inner cotyledon and radicle showed lower labelling. Epidermis and provascular tissues were also labelled.

(**I**) Schematic representation of oleosin distribution according to immunostaining analysis.

Abbreviations: al: aleurone layer, cc: central cylinder, en: endosperm, ic: inner cotyledon, oc: outer cotyledon, sc: seed coat.

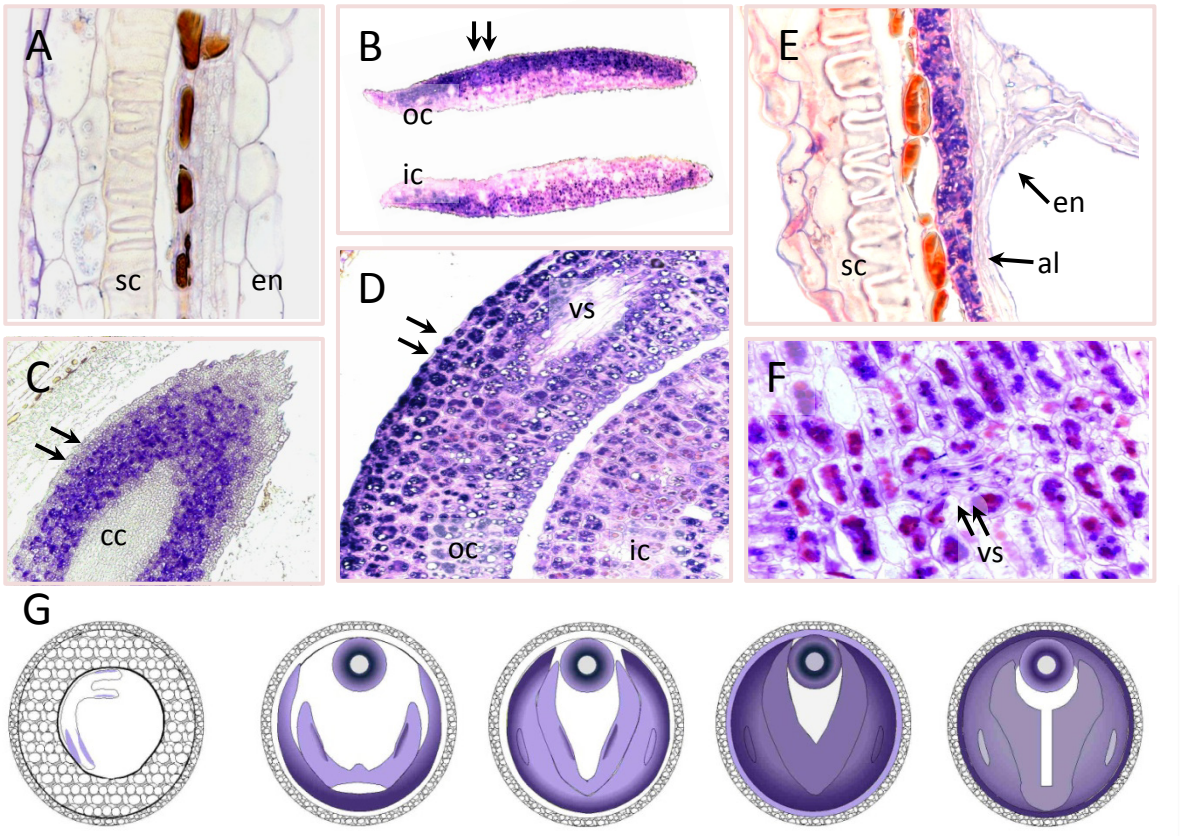

Supplemental Figure 3. Spatial and temporal pattern of napin accumulation in developing seeds of *B. napus* analysed by immunostaining.

(**A-B**) early stage: labelling detected deposition of protein in embryo while both seed coat and endosperm were not labelled (A). Accumulation of napin started at the tip of the axis (radicle), and spread toward cotyledons (not shown). Cotyledons were stained starting from the base and mainly within abaxial region (arrowed in B). The inner cotyledon was less intensely stained.

(**C-D**) mid stage: neither seed coat nor endosperm were labelled. Immunolabelling was observed in embryo only. It localised mainly within parenchyma of cortex (arrowed in C). Both cotyledons were stained: outer cotyledon showed strong gradient with maximum within abaxial region (arrowed in D). Gradient within the inner cotyledon was less pronounced. Stained protein bodies were detectable within epidermis. Provascular tissue was not labelled.

(**E-F**) late stage: labelling appeared in aleurone layer of epidermis (E). In embryo, intensity of labelling reached its maximum. Gradient in staining was observed within outer cotyledon, while the inner cotyledon and radicle were less intensely stained (not shown). Epidermis and provascular tissues were also labelled (F).

(**G**) Schematic representation of napin distribution according to immunostaining analysis.

Abbreviations: al: aleurone layer, cc: central cylinder, en: endosperm, ic: inner cotyledon, oc: outer cotyledon, sc: seed coat, vs: vascular tissue.

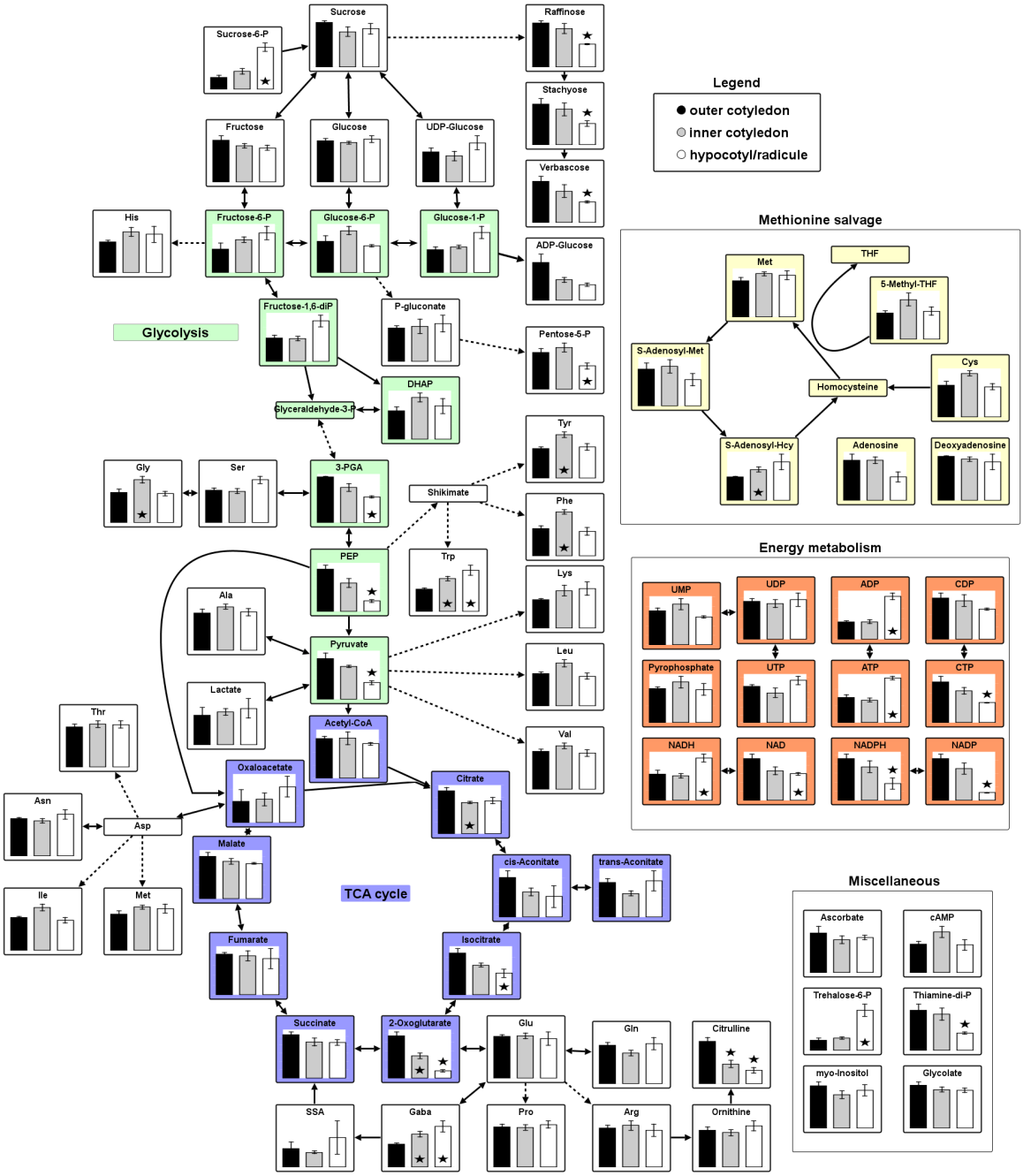

Supplemental Figure 4. Metabolite distribution in various organs of the *B. napus* embryo (30 DAF).

Steady state metabolite levels were measured in dissected organs by LC/MS. Data are in the form of mean ± SE (n=5), and are listed in Suppl. Dataset 4A. Colours indicate various pathways and stars indicate statistically significant ($p<0.05$) differences according to a *t*-test. Abbreviations: 3-PGA = 3-phosphoglycerate; PEP = phosphoenolpyruvate; SSA = succinic semialdehyde; Gaba = γ-aminobutyric acid; THF = tetrahydrofolate; cAMP = cyclic AMP.

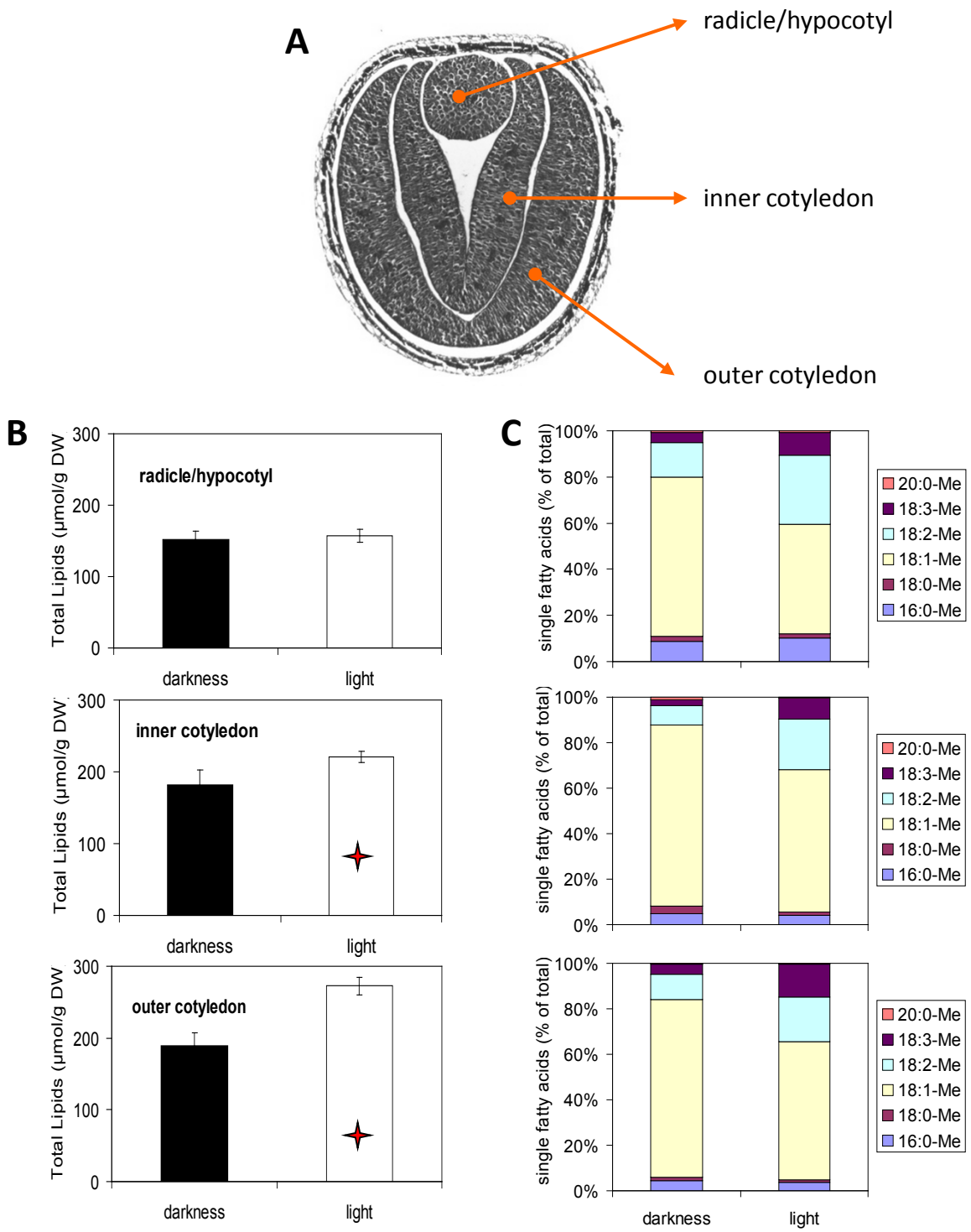

Supplemental Figure 5. Effect of pod shading on lipid content and fatty acid composition in various components of the *B. napus* embryo.

(**A**) Scheme showing the various organs dissected by hand and used for analysis of lipids.

(**B**) Total lipid content in various organs grown under lit and non-lit conditions. Error bars indicate standard deviation. Stars indicate statistically significant differences versus dark treatment (n=6; t-test; $p<0.05$).

(**C**) Fatty acid composition in various embryo organs grown under lit and non-lit conditions (n=6).

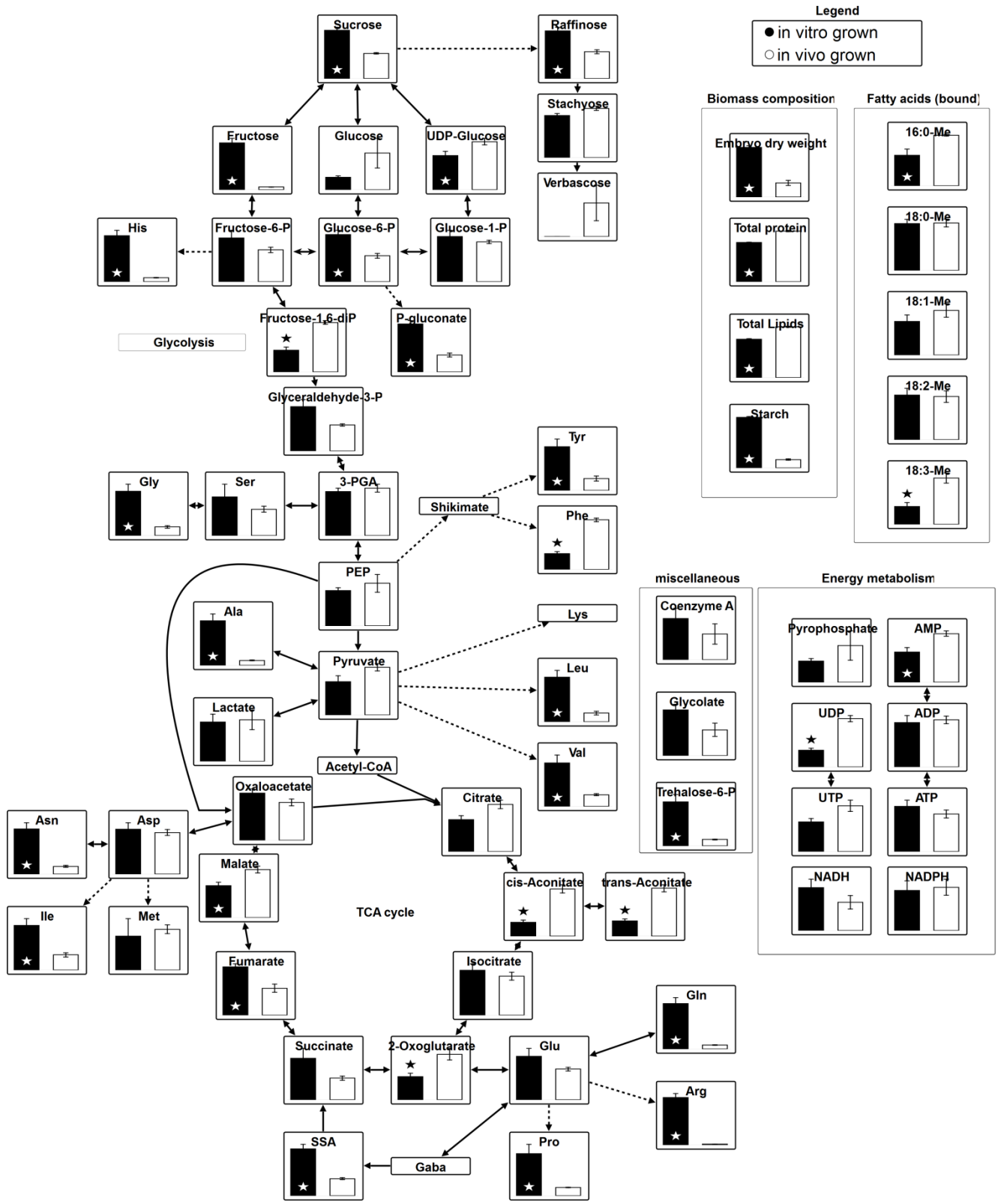

Supplemental Figure 6. Comparison of biomass composition and steady state metabolite levels of *B. napus* embryos grown *in planta* versus *in vitro*. Error bars indicate standard deviation. Stars indicate statistically significant differences according to t-test ($p<0.05$)